ACS APPLIED MATERIALS & INTERFACES

Research Article

www.acsami.org

Size-Dependent Stability of Water-Solubilized CdTe Quantum Dots and Their Uptake Mechanism by Live HeLa Cells

Tiantian Wang[†,‡] and Xiue Jiang*[,†]

[†]State Key Laboratory of Electroanalytical Chemistry, Changchun Institute of Applied Chemistry, Chinese Academy of Sciences, Changchun 130022, China

[‡]Graduate University of Chinese Academy of Sciences, Beijing 100049, China

Supporting Information

ABSTRACT: Water-solubilized quantum dots have led to a promising application in cellular labeling and biological imaging. The physicochemical properties of water-solubilized quantum dots, particularly in a physiological environment, are strongly dependent on their size. In this paper, we systematically studied the stability of mercaptosuccinic acid-coated CdTe quantum dots (MSA-QDs) of about 2.3 and 5.4 nm diameters in various buffers with different pH values and under laser irradiation by fluorescence spectroscopy. It was found that larger MSA-QDs showed better stability. Size-dependent uptake of MSA-QDs by living HeLa cells was further investigated by confocal microscopy. In phosphate buffer solution, the larger MSA-QDs entered the cells mainly by endocytosis, and part of the smaller ones entered the cells by passive penetration. In cell culture medium, their uptake pathways could be changed due to the changes of their surface properties. The cytotoxicity of smaller and larger MSA-QDs was significantly decreased due to the adsorption of some biological components in the cell culture medium on the nanoparticles surface.

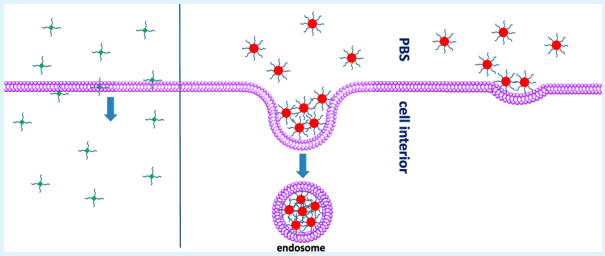

KEYWORDS: *CdTe quantum dots, size-dependent stability, uptake mechanism, small diameter, confocal microscopy, fluorescence spectroscopy*

1. INTRODUCTION

The use of engineered nanoparticles in medical, cosmetic, or food products has been rapidly expanding,[1−4] which inevitably increases the chance of human exposure to nanoparticles. Their small size enables them to penetrate physiological barriers and invade living organisms.[5] Upon nanoparticle exposure, cells incorporate nanoparticles either by endocytosis, i.e., actively going with vesicle formation, or by passive penetration, generally driven by concentration gradient.[6−12] The efficiency of nanoparticle uptake and the uptake mechanisms by live cells are determined by size,[13−17] shape,[13,15] surface charge,[18−25] and surface modification of nanoparticles.[7,26] A profound understanding of the relationship between the physicochemical properties of nanoparticles and the elicited cellular uptake is a prerequisite for their safe and beneficial use.

Among these factors, size may be the dominating one, because the small size enables them to overcome or even avoid various biological barriers. Although many investigations about size-dependent cellular uptake of nanoparticles with diameter of more than 10 nm have been reported,[13−17] little is known in the range of about 5 nm, except that Maysinger et al. have investigated the subcellular distribution and toxicity of positively charged CdTe quantum dots (QDs) of about 2 and 5 nm diameter.[10] The physicochemical properties of small nanoparticles are easily affected in biological milieu.[27,28] Many studies also suggested that the potential cytotoxicity induced by the accumulation of nanoparticles inside live cells is highly related to the physicochemical properties of nanoparticles,[29−33] such as the size, surface chemistry, and stability. The release of heavy metals into cytosol may result in the production of reactive oxygen intermediates (ROI).[30]

Owing to their small size and multicolored property, colloidal semiconductor quantum dots are good candidates used to investigate the size-dependent uptake mechanism of nanoparticles with diameter of about 5 nm. Colloidal semiconductor core/shell quantum dots have been extensively applied in biomedicine.[34,35] However, synthesis of core/shell particles in organic phases and translocation of hydrophobic core/shell nanoparticles into aqueous solution by ligand-exchange inevitably increase the diameter of the nanoparticles; therefore, it is difficult to get nanoparticles with various diameters in the range of about 5 nm. Aqueous synthesis of CdTe nanoparticles with small ligand as stabilizer makes it easy to get various diameters in the range of about 5 nm.[36,37]

In this work, we systematically studied the size-dependent stability of mercaptosuccinic acid-capped CdTe QDs in various buffers, cell culture medium, and under laser irradiation. The cytotoxicity of the particles was also evaluated by MTT assay. The size-dependent uptake mechanism of negatively charged CdTe QDs was studied by incubating QDs with HeLa cells.

Received: February 18, 2012
Accepted: December 13, 2012
Published: February 6, 2013

Our results revealed that the size of the nanoparticles is a predominant determinant for their stability and the way of entering cells. The results may be contributory for understanding the cytotoxicity of nanomaterials with small size and improving the security of their applications in biology.

2. EXPERIMENTAL SECTION

Synthesis of Mercaptosuccinic Acid-Capped CdTe QDs and Physicochemical Properties. The mercaptosuccinic acid-capped CdTe QDs (MSA-QDs) were prepared according to the method of previously published procedures.[36,37] Briefly, cadmium chloride ($CdCl_2$) of 0.04 mol L^{-1} in 4 mL of aqueous solution was diluted to 50 mL in a one-necked flask, and then 100 mg of trisodium citrate dihydrate, 4 mL of 0.01 mol L^{-1} sodium tellurite (Na_2TeO_3, Aldrich) aqueous solution, 50 mg of mercaptosuccinic acid (MSA, Aldrich), and 50 mg of sodium borohydride ($NaBH_4$) were added together into the one-necked flask under stirring. When the solution changed to yellow color, the flask was attached to a condenser and refluxed at 100 °C under open-air conditions. The size of formed nanoparticles could be tuned by controlling the reflux time and easily monitored by absorption and photoluminescence (PL) spectra.

After reflux for about 1.5 and 12 h, green and red-emitting MSA-QDs were obtained, respectively. MSA-QDs solution was mixed with absolute alcohol at a volume ratio of 1:3 and separated by centrifugation at 6640*g* for 20 min. The precipitation was evaporated in a vacuum case and then dissolved in phosphate buffered saline (PBS, pH = 7.4) as a stock solution and kept at 4 °C. The UV−vis absorption and PL spectra of both QDs were recorded by a Cary 500 Scan UV−visible spectrophotometer (Varian, U.S.A.) and a Fluoromax-4 spectrofluorometer (Horiba Jobin Yvon Inc., France), respectively. The green MSA-QDs show an intensive absorption at 530 nm from the first electronic transition and a strong emission centered at 549 nm with an excitation wavelength of 400 nm. The red ones show an intensive absorption at 595 nm and an emission centered at 624 nm with the excitation wavelength of 488 nm. The hydrodynamic sizes of synthesized green and red MSA-QDs characterized by fluorescence correlation spectroscopy using a home-built setup[38] are 2.3 ± 0.2 and 5.4 ± 0.2 nm, respectively. ζ-potential determined in aqueous solution by dynamic light scattering using a Zetasizer (ZEN3600, Malvern co., UK) is −20.05 ± 1.63 and −16.48 ± 1.04 mV, respectively for the green and red MSA-QDs. All data are compiled in Table 1. Although the zeta potential of the two particles is not the same, they are both negative and the gap is little. Thus, the main difference of the two types of MSA-QDs should be the size.

Table 1. Physicochemical Properties of Quantum Dots

quantum dots	λ_{abs} (nm)[a]	λ_{em} (nm)[b]	ζ-potential (mV)	diameter (nm)
red	595	624	−16.48 ± 1.04	5.4 ± 0.2
green	530	549	−20.05 ± 1.63	2.3 ± 0.2

[a]Typical absorption band. [b]Emission maximum.

Stability Experiment in Buffers, Cell Culture Medium, and under Laser Irradiation. Sorensen's phosphate buffer solutions (PBS) of pH varied from 6.02 to 8.32 were prepared by mixing 66.7 mM Na_2HPO_4 and KH_2PO_4 solutions at different ratios. The buffer solution of pH = 3.66 and 4.80 was prepared with 0.1 M citric acid and 0.1 M sodium citrate solutions mixed at the ratio of about 2:1 and 1:1, respectively. The Tris−HCl buffer solution of pH = 9.05 was prepared by mixing 7.0 mL of 0.1 M HCl solution to 50 mL of 0.1 M tris(hydroxy methyl)aminomethane (Tris) solution and adding water to 100 mL. Dulbecco's modified eagle medium (DMEM, Invitrogen Corporation), either supplemented with 10% fetal bovine serum (Tianjin Hanyang Biologicals Technology Co., Ltd., China) or not, was used as cell culture medium. The PL spectrum was measured as soon as MSA-QDs were injected into the buffer solutions or cell culture medium and every several hours.

In addition, the green (114 μg mL^{-1}, left) and the red (356 μg mL^{-1}) MSA-QDs dissolved in PBS (pH = 7.24) were injected into a microcell and irradiated by an Ar^+ ion laser giving the excitation line of 514.5 nm equipped in Renishaw 2000 (Renishaw Co., United Kingdom). The power of the laser beam was estimated to be about 25 mW. After irradiation for a period of time, the PL spectrum was recorded.

Cell Culture and Cellular Images. HeLa cells were cultured in DMEM, supplemented with 10% fetal bovine serum and 1% penicillin−streptomycin solution (100×) (Beyotime Institute of Biotechnology, China) in a humidified incubator at 37 °C, 5% CO_2, and were seeded in a 35 mm tissue culture dish (NEST Biotech Co., Ltd., China) at a density of 32 000 cells. Cells were allowed to adhere overnight before they were rinsed three times with PBS. For nanoparticle uptake experiments, cells were incubated with 800 μL of MSA-QDs at a concentration of 8 μg mL^{-1} in PBS by solution exchange unless stated otherwise. The cells were imaged over 2 h at selected times using a confocal laser scanning fluorescence microscope (CLSM, Leica TCS SP2, Leica Microsystems, Mannheim, Germany) with 100× objective accompanied with CO_2 and temperature control (37 °C and 5% CO_2 PECON, Erbach, Germany). Nanoparticles were excited with an Ar^+ ion laser giving the excitation line of 488 nm and observed through 586−649 and 505−568 nm emission bandpass filters for the red and green MSA-QDs, respectively.

Alternatively, before MSA-QDs addition, the cells were preincubated at 4 °C for 50 min. The PBS for MSA-QDs incubation and wash and the MSA-QDs stock solutions were all preincubated to 4 °C before use. Control sample cells without incubation with MSA-QDs were also imaged. The mean fluorescence intensities at 4 °C were obtained by image J software with the function of time series analyzer V20.

Cell Viability Assay. The viability of cells after exposure to MSA-QDs was investigated by MTT assay. HeLa cells were seeded in a 96-well plate at a density of 10 000 cells per well, and the plate was kept in a 5% CO_2 incubator at 37 °C for 2 days. After that, the cells were exposed to 200 μL of QDs in PBS or in cell culture medium with the concentration of 8 μg mL^{-1} for a certain time (2, 5, and 24 h) in 5% CO_2 at 37 °C. A control experiment was performed in the absence of QDs similarly. After washing 3 times with PBS, 100 μL of medium and 10 μL of MTT (5 mg mL^{-1}) were added in each well followed by incubation for 4 h. The precipitated formazan violet crystals were dissolved by 150 μL of dimethylsulfoxide (DMSO, Sigma), and the absorbance values were monitored using PowerWave XS2 microplate reader (Gen 5, BioTek, USA) at 555 nm. Due to the low concentration of the used QDs, the absorption of both of the two types of QDs was too low to be detected, so the interference of the nanoparticles was negligible. The percentage of live cells was calculated according to $A_{555\ nm}/A_{555\ nm\ (Control)}$.

3. RESULTS AND DISCUSSION

Photochemical Instability of MSA-QDs in Aqueous Solution. The water-soluble semiconductor QDs have attracted much attention as probes for in vitro and in vivo imaging. Therefore, the evaluation of the photochemical stability is necessary for their successful applications. The size-dependent photochemical instability of MSA-QDs was evaluated in pH 7.24 PBS. The PL spectra of the green and the red MSA-QDs aqueous solution were recorded after different irradiation time by 514.5 nm Ar ion laser with the power of about 25 mW. As shown in Figure 1, with prolonging irradiation time, the maximum intensities of the PL spectra of both MSA-QDs decrease. This indicates that neither the green nor the red MSA-QDs are stable under the continual illumination with high power laser. The photochemical instability of CdSe nanoparticles coated by hydrophilic thiols has been found to be caused by photocatalytic oxidation of the thiol ligands, the photooxidation of CdSe nanocrystals, and the

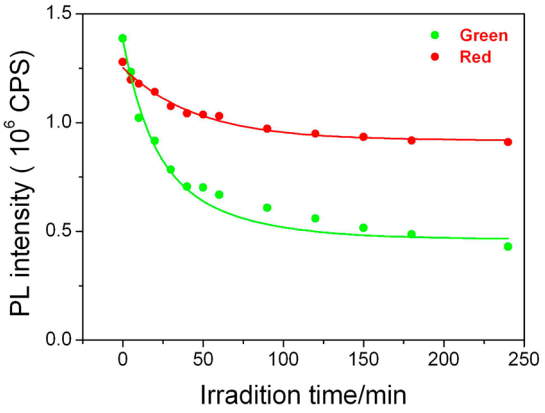

Figure 1. Photobleaching curves of the green (114 μg mL^{-1}) and the red (356 μg mL^{-1}) MSA-QDs in pH 7.24 PBS under laser irradiation.

precipitation of the nanocrystals.[39] The smaller nanocrystals are oxidized more rapidly than the larger ones.[39] The photooxidation breaks the surface Cd−S bond during the laser irradiation. The loss of thiol ligands would produce defects on the QD surface, resulting in the decrease of the PL intensity of the QDs as photobleaching.[28] The green MSA-QDs are smaller than the red ones. With the decrease of nanoparticles size from 5.4 to 2.3 nm, the specific surface area is increased significantly, which results in more free coordination places at the surface due to the increase of the surface atom. Since irradiation-induced quenching of MSA-QDs is the result of photooxidation by dissolved oxygen, smaller MSA-QDs with more free coordination places at the surface would increase their interactions with dissolved oxygen and result in stronger photooxidation. Therefore, the green MSA-QDs showed less stability than the red ones under laser irradiation. Boldt et al. have studied the stability of CdTe QDs capped by thioglycolic,[28] they found that smaller QDs were more stable, which might suggest the stability of CdTe QDs are also ligand dependent.

Stability of MSA-QDs in Buffers and Cell Culture Medium. Detailed investigation of the physicochemical properties of small QDs in physiological conditions is also a prerequisite for the application of nanoparticles in biomedicine because exposure of nanoparticles to the biological fluids might change their properties due to the change of local pH and the adsorption of biological components. Therefore, we systematically studied the size-dependent stability of MSA-QDs in various buffers with different pH values and in cell culture medium.

We mixed both MSA-QDs with different pH buffer solutions and recorded the PL spectra in 24 h, respectively. The maximum intensity of each emission spectrum was plotted as a function of the measurement time. As shown in Figure 2, the PL intensity of the green and the red MSA-QDs remains nearly constant in the pH range from 6.02 to 9.05, which indicates that both MSA-QDs are stable in neutral and alkalescent buffer solutions. Upon shift of the pH value to lower than 5, the PL intensity of both QDs dropped with time with different rates. In pH 3.66, the PL intensity of the green MSA-QDs dropped to 50% in 0.7 h, while the PL intensity of the red MSA-QDs dropped to 50% in 5 h. This indicates that the red MSA-QDs exhibit better stability than the green ones. A previous report has proved that the coordination between the carbonyl O atom of free mercaptocarboxylic acid and the Cd atom at the CdTe surface could stabilize the CdTe QDs at low pH.[40,41] In comparison with the red MSA-QDs, smaller green MSA-QDs have bigger curvature radius, which should weaken the coordination interactions. This might result in their less stability.

For evaluating the size-dependent stability of MSA-QDs in biological fluid, we also measured the PL spectra of both MSA-QDs mixed with DMEM in the absence or presence of fetal bovine serum (FBS). In the absence of FBS, the maximum PL peak of the green MSA-QDs at 549 nm was completely quenched with the appearance of a new peak at 578 nm as soon as MSA-QDs were mixed with DMEM (Figure 3). To ascertain the component in DMEM which led to the reduced PL intensity, we checked the fluorescence compositions in DMEM. The fluorescence of DMEM mostly comes from lactoflavin, phenol red, and folic acid. We separately prepared their solution according to their concentration in DMEM and incubated MSA-QDs with the above solution, respectively. The pH of these solutions was the same as the cell culture medium, about 7.4. We found that only phenol red could dramatically quench the PL intensity of the green MSA-QDs. To confirm the effect of phenol red, we added $Na_2S_2O_4$ to the solution to reduce phenol red. After addition of $Na_2S_2O_4$ to the green MSA-QDs solution containing phenol red, the PL intensity of the green MSA-QDs could recover to original intensity as shown in Figure S1 (Supporting Information). Therefore, we deduced that the quenching of the phenol red to the QDs

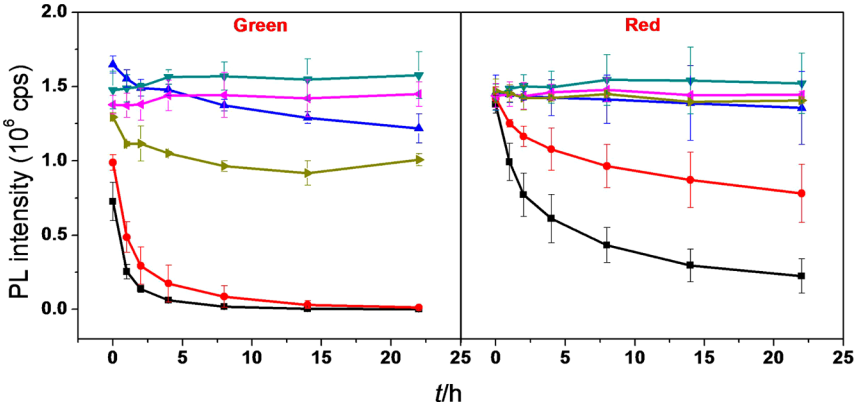

Figure 2. Time-dependent photoluminescent intensities of the green (114 μg mL^{-1}, left) and the red (356 μg mL^{-1}) MSA-QDs in buffer solutions with pH value of 3.66 (black), 4.8 (red), 6.02 (blue), 7.24 (dark cyan), 8.32 (magenta), and 9.05 (dark yellow).

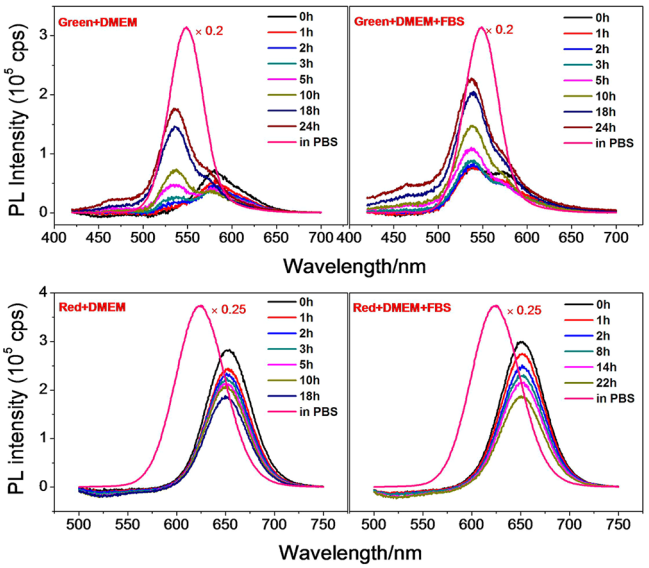

Figure 3. Time-dependent luminescent spectra of the green (114 μg mL^{-1}) and the red (356 μg mL^{-1}) MSA-QDs in DMEM without (left panel) and with (right panel) FBS compared with their fluorescence spectra in PBS (pH 7.24) as control.

should come from the electron transfer of QDs to the phenol red. On the basis of these results, we can ensure that phenol red was the main quencher. However, sole phenol red did not quench the fluorescence of MSA-QDs as much as that in DMEM, which suggests the role of other components, such as surfactant in DMEM. However, due to the multiple components in DMEM, it is difficult to exactly identify the surfactant that completely quenched the PL intensity of the green MSA-QDs together with the phenol red. As the time proceeded, the peak at 578 nm dropped off and the peak of the green MSA-QDs appeared again but shifted to 535 nm with gradual increase in intensity. This might suggest the existence of a balance between the adsorption and desorption. The blue shift should be the result of a partial destruction of the green MSA-QDs when adsorbed substance was desorbed from the surface.[28] It is worth noting that, in the presence of FBS, the PL peak of the green QDs still remained at a certain intensity with a shoulder peak at 578 nm. Such apparent difference suggests the adsorption of proteins to the green MSA-QDs, and the adsorbed protein affected the action of the quencher.

For the red MSA-QDs, their PL intensity was also dramatically decreased, but their peak position was shifted from 624 to 650 nm as soon as they were mixed with DMEM; then,the PL intensity gradually decreased with time. Similarly, we also identified that the phenol red is the main quencher (Supporting Information, Figure S1). However, unlike the green MSA-QDs, addition of FBS to DMEM had no effect on the changes of the red MSA-QDs fluorescence. This indicates that the proteins of the FBS were not adsorbed to the red MSA-QDs, or the adsorbed protein had no effect on the action of the quencher. To further identify if the protein was adsorbed on the red MSA-QDs, we observed the effect of both MSA-QDs on the fluorescence of FBS in DMEM (Supporting Information, Figure S2). Obviously, addition of both QDs caused a noticeable decrease in FBS fluorescence intensity, suggesting the interaction of proteins of FBS with both MSA-QDs. However, the adsorbed proteins did not change the effect of the quencher on the fluorescence emission of the red MSA-QDs, which might suggest that proteins bind indirectly to the molecules on the particle surface. The red shift might be the results of additional sulfuration reactions on the QDs surface from the component of DMEM.[28] Adsorption of the components in cell culture medium also dramatically affected the surface charge of both MSA-QDs since the zeta potential of both MSA-QDs dramatically decreased (Figure S3, Supporting Information). However, there is no significant difference in the zeta potential of both QDs in cell culture medium, and the varied tendency is similar. This excludes the effect of surface charge on the size-dependent stability of both QDs.

Uptake of MSA-QDs by Live HeLa Cells. In order to study the details of the size-dependent uptake of MSA-QDs by HeLa cells, we incubated HeLa cells with both MSA-QDs at a concentration of 8 μg mL^{-1} dissolved in PBS buffer, respectively. The green and red MSA-QDs have nearly the identical PL intensity at the concentration of 8 μg mL^{-1} under excitation at 488 nm (Supporting Information, Figure S4). The spatial distribution of the MSA-QDs by imaging planes through the cells at about half height during 2 h of exposure was recorded using a confocal microscope. Figure 4 shows, as an example, uptake of the green (panel a) and the red (panel b) MSA-QDs by HeLa cells at selected times after nanoparticles exposure. Apparent internalization of the green MSA-QDs by HeLa cells is already visible after a 10 min incubation. A gradual accumulation thereafter is observed, seen as continuous enrichment of bright visible objects, which are distributed in the cytoplasm after 70 min as seen from the overlay images (Figure 4a). The green signal is not enhanced near the cell

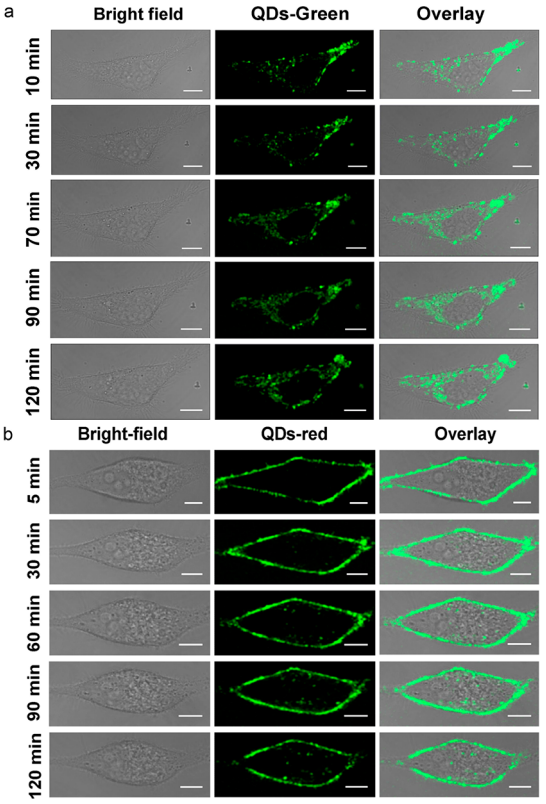

Figure 4. Confocal images of HeLa cells exposed to the green (a) and the red (b) MSA-QDs with a concentration of 8 μg mL^{-1} in PBS at different incubation times. The experiments were completed under living cell condition (37 °C, 5% CO_2). Scale bar: 10 μm.

dx.doi.org/10.1021/am302234z | ACS Appl. Mater. Interfaces 2013, 5, 1190−1196

membrane and in the nuclear region even after 2 h. In contrast, after exposure of the cells to the red MSA-QDs, the green signal is enhanced near the cell membrane within 3 min and the intensity increased gradually. However, no obviously bright spots are observed inside the cells until a 30 min incubation. After that, a gradual accumulation is observed, seen as continuous enrichment of bright spots, which accumulate as particle clusters. Fluorescence is also not significantly enhanced in the nuclear region. Such apparent difference should suggest that the size-dependent uptake mechanisms are different. We have noted that uptake of smaller zwitterionic quantum dots of 8 nm diameter involved binding to the cell membrane.[42] Prior to endocytosis, the small QDs strongly accumulated on the plasma membrane.[42] Membrane-attached nanoparticles trigger the diffusion of receptors into the binding site to bind with the nanoparticles, which induces the membrane wraps around the particles[6] prior to the endocytosis. For small nanoparticles, only if a sufficiently large cluster of nanoparticles are packaged locally, can complete wrapping occur.[42] Obviously, accumulation of the red MSA-QDs on the cell membrane is a prerequisite for endocytosis. In contrast, no membrane accumulation of the green MSA-QDs might suggest a different uptake mechanism. It has been reported that green cationic QDs, SiO_2 nanoparticles, and gold particles of various sizes coated with cargo-receptor complexes could penetrate through the cellular membrane and enter the nucleolus.[26,43,44] The faster uptake rate and lacking accumulation of the green MSA-QDs at the cellular membrane might suggest that the nanoparticles enter the cells by passive penetration. Due to the restricted channels in the nuclear membrane, in comparison to the plasma membrane, the nuclear membrane cannot easily be traversed. Although the nuclear pore complexes allow passive diffusion of molecules through aqueous channels with a diameter of 9 nm, the easy association of the green and red MSA-QDs with biological components in the cytoplasm will inevitably enlarge the diameter of both MSA-QDs and impede their penetration to the nuclear membrane.

To further identify the size-dependent uptake mechanism of small CdTe nanoparticles by living HeLa cells, we have carried out uptake inhibition experiments at 4 °C. HeLa cells preincubated at 4 °C for 50 min were imaged as control (Figure 5a). The green and the red MSA-QDs were added to precooled HeLa cells, respectively, and kept at 4 °C for 90 min. Representative confocal images are shown in Figure 5. The red MSA-QDs only accumulated on the cell membrane and did not enter the cells, indicating that HeLa cells incorporated the red MSA-QDs by active endocytosis, because at 4 °C, active uptake processes have been practically arrested. However, some green MSA-QDs entered the cells, supported by quantitative image analysis (Figure 5b). Mean intensity was obtained by calculating the integrated fluorescence intensity of the intracellular region, normalizing them to the cellular area, and subtracting the mean intensity of the background. The mean intensity calculated by entrance of the green MSA-QDs is significantly different from the control, indicating that part of the green MSA-QDs entered the cells by passive penetration. It should be noted that some green MSA-QDs still enter the cells through active endocytosis, since part of the accumulation of the green QDs is at the cellular membranes.

Cell Toxicity Evaluation. To exclude the effect of the cytotoxicity on the difference of uptake mechanism, we studied the cytotoxicity of the two types of MSA-QDs by MTT assay. Treating the HeLa cells with 8 μg mL^{-1} green and red MSA-QDs for 2 h in PBS did not induce significant effect on the cell viability in comparison to control (Figure 6). Even after a 5 h incubation, still, greater than 80% of cells were alive after treating with both MSA-QDs. This excludes the effect of cytotoxicity on the difference of both MSA-QDs in their uptake mechanism since our observation was limited to 2 h. After a 24 h incubation in PBS, the cytotoxicity was obvious. Only less than 30% of cells were alive, but if the QDs were dissolved in cell culture medium with 10% FBS and the mixture was incubated with HeLa cells for 24 h, almost no cytotoxicity was observed. Thus, to a certain extent, some biological components adsorbed on the surface of QDs inhibited the toxicity of the QDs. The adsorbed components might inhibit the release of ions. Besides, we also analyzed the membrane

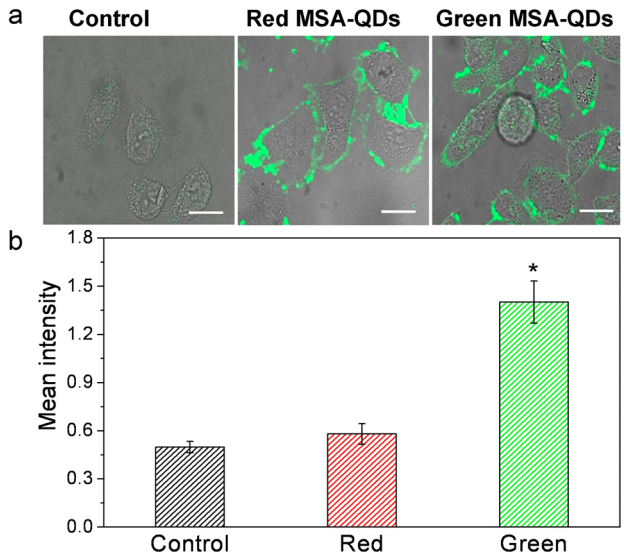

Figure 5. (a) Confocal images of HeLa cells exposed to the green and the red MSA-QDs (8 μg mL^{-1}) for 90 min in PBS at 4 °C relative to untreated cells with MSA-QDs as a control. Scale bar: 20 μm. (b) Mean fluorescence intensities from confocal images at 4 °C, averaged from 30 cells in two different experiments; error bars indicate standard deviations from the mean. The statistically significant difference ($p < 0.05$) between green MSA-QD-treated HeLa cells and untreated cells is indicated by the asterisk.

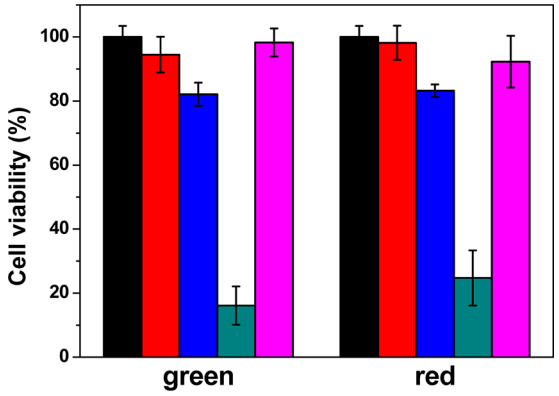

Figure 6. Effect of the green and red MSA-QDs at 8 μg mL^{-1} on the viability of HeLa cells, incubating with HeLa cells about 2 h (red), 5 h (blue), 24 h in PBS (dark cyan), and 24 h in cell culture medium (magenta), as quantified by MTT assay. The black column is the control experiment.

integrity of cells after exposure of cells to QDs (Figure S5, Supporting Information). Propidium iodide (PI) was added to the HeLa cells after incubation for 2 h with both MSA-QDs. After addition of PI for 15 min, the nuclear staining was not observed, indicating intact plasma membrane. This further excludes the effect of cytotoxicity on the difference of both MSA-QDs in their uptake mechanism.

Incubation of MSA-QDs with cell culture medium has been shown to significantly decrease the cytotoxicity due to the adsorption of biological components on nanoparticles surface. We therefore checked if such change will affect the cellular uptake. Compared with bare green MSA-QDs in PBS, incubation of the green MSA-QDs in DMEM with 10% FBS resulted in part accumulation of the green MSA-QDs on the cell membrane and the decrease of intracellular uptake (Figure 7). The membrane-associated QDs were substantially reduced

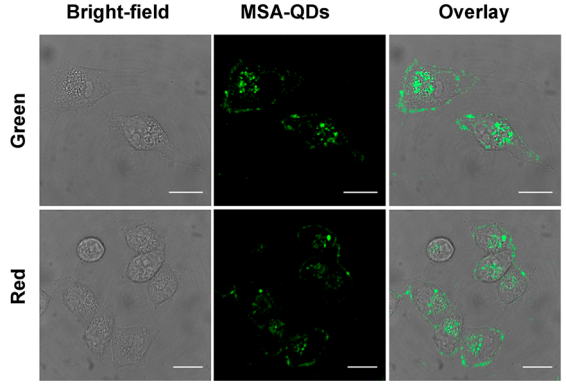

Figure 7. Confocal images of HeLa cells exposed to 8 μg mL^{-1} green and red MSA-QDs in DMEM supplied with 10% FBS for 90 min. MSA-QDs were mixed with cell culture medium for 24 h prior to use. The experiments were completed under living cell condition (37 °C, 5% CO_2). Scale bar: 10 μm.

for the red MSA-QDs (Figure 7). These differences indicate that adsorption of some components in cell culture medium to the surface of MSA-QDs obviously changes their internalization pathway by living HeLa cells. The obvious decrease in the cellular uptake for both MSA-QDs should also decrease the cytotoxicity.

4. CONCLUSIONS

Detailed investigation of the physicochemical properties of small nanoparticles in physiological conditions, their uptake mechanism by living cells, and their cytotoxicity are prerequisites for their application in biomedicine. In this work, we systematically studied the size-dependent photostability of small MSA-QDs under laser irradiation and in various buffers and cell culture medium by fluorescence spectroscopy. The larger MSA-QDs exhibited better stability in acidic buffer solution and under laser irradiation due to the effect of their curvature radius and specific surface area. In cell culture medium, the luminescent intensity of both MSA-QDs was quenched distinctly due to the adsorption of phenol red and other components but in different manners dependent on size. The quenched PL intensity of the green MSA-QDs could be partly recovered accompanied by the destruction of the nanoparticles. In contrast, the adsorbed components on the red MSA-QDs continually quenched the PL intensity of the red QDs. Size-dependent uptake mechanism of MSA-QDs in PBS and cell culture medium was studied by confocal microscopy. When incubated with HeLa cells in PBS, the red MSA-QDs entered the cells mainly by active endocytosis, but part of the green MSA-QDs entered the cells by passive penetration. Both bare MSA-QDs resulted in significant cytotoxicity after coincubation with live HeLa cells in PBS for 24 h. This can be avoided by coincubation of both QDs with live HeLa cells in cell culture medium.

■ ASSOCIATED CONTENT

Supporting Information

Impact of phenol red on the PL intensity of the green and red MSA-QDs. Study of the interactions of both MSA-QDs with proteins of FBS. Time-dependent zeta potential in cell culture media for the green and red MSA-QDs. Fluorescence spectra measurements for quantitation of the PL intensity of both MSA-QDs. Confocal images of HeLa cells for analyzing the membrane integrity. This information is available free of charge via the Internet at http://pubs.acs.org/.

■ AUTHOR INFORMATION

Corresponding Author

*Phone: +86 431 85262426. Fax: +86 431 85685653. E-mail: jiangxiue@ciac.jl.cn.

Notes

The authors declare no competing financial interest.

■ ACKNOWLEDGMENTS

This work was supported by the President Funds of the Chinese Academy of Sciences, Youth Foundation of China (21105097), Youth Foundation of Jilin Province (201101081), Startup Foundation for Scientific Research, and Changchun Institute of Applied Chemistry, Chinese Academy of Sciences.

■ REFERENCES

(1) Grobe, A.; Renn, O.; Jaeger, A. Available from: http://www.nanowerk.com/nanotechnology/reports/reportpdf/report125.pdf (Accessed Feb. 26, 2010).
(2) Liu, J.; Lau, S. K.; Varma, V. A.; Kairdolf, B. A.; Nie, S. *Anal. Chem.* **2010**, *82*, 6237−6243.
(3) Maesaki, S. *Curr. Pharm. Des.* **2002**, *8*, 433−440.
(4) Lewin, M.; Carlesso, N.; Tung, C.-H.; Tang, X.-W.; Cory, D.; Scadden, D. T.; Weissleder, R. *Nat. Biotechnol.* **2000**, *18*, 410−414.
(5) Colvin, V. L. *Nat. Biotechnol.* **2003**, *21*, 1166−1170.
(6) Nel, A. E.; Mädler, L.; Velegol, D.; Xia, T.; Hoek, E. M. V.; Somasundaran, P.; Klaessig, F.; Castranova, V.; Thompson, M. *Nat. Mater.* **2009**, *8*, 543−557.
(7) Jiang, X.; Dausend, J.; Hafner, M.; Musyanovych, A.; Röcker, C.; Landfester, K.; Mailänder, V.; Nienhaus, G. U. *Biomacromolecules* **2010**, *11*, 748−753.
(8) Jiang, X.; Weise, S.; Hafner, M.; Röcker, C.; Zhang, F.; Parak, W. J.; Nienhaus, G. U. *J. R. Soc. Interface* **2010**, *7*, S5−S13.
(9) Verma, A.; Stellacci, F. *Small* **2010**, *6*, 12−21.
(10) Lovrić, J.; Bazzi, H. S.; Cuie, Y.; Fortin, G. R. A.; Winnik, F. M.; Maysinger, D. *J. Mol. Med.* **2005**, *83*, 377−385.
(11) Verma, A.; Uzun, O.; Hu, Y.; Hu, Y.; Han, H.-S.; Watson, N.; Chen, S.; Irvine, D. J.; Stellacci, F. *Nat. Mater.* **2008**, *7*, 588−595.
(12) Choleris, E.; Little, S. R.; Mong, J. A.; Puram, S. V.; Langer, R.; Pfaff, D. W. *Proc. Natl. Acad. Sci. U. S. A* **2007**, *104*, 4670−4675.
(13) Rejman, J.; Oberle, V.; Zuhorn, I. S.; Hoekstra, D. *Biochem. J.* **2004**, *377*, 159−169.
(14) Chithrani, B. D.; Ghazani, A. A.; Chan, W. C. W. *Nano Lett.* **2006**, *6*, 662−668.
(15) Chithrani, B. D.; Chan, W. C. W. *Nano Lett.* **2007**, *7*, 1542−1550.

(16) Lai, S. K.; Hida, K.; Man, S. T.; Chen, C.; Machamer, C.; Schroer, T. A.; Hanes, J. *Biomaterials* **2007**, *28*, 2876−2884.
(17) He, C.; Hu, Y.; Yin, L.; Tang, C.; Yin, C. *Biomaterials* **2010**, *31*, 3657−3666.
(18) Arbab, A. S.; Bashaw, L. A.; Miller, B. R.; Jordan, E. K.; Bulte, J. W. M.; Frank, J. A. *Transplantation* **2003**, *76*, 1123−1130.
(19) Oyewumi, M. O.; Yokel, R. A.; Jay, M.; Coakley, T.; Mumper, R. J. *J. Controlled Release* **2004**, *95*, 613−626.
(20) Sun, R.; Dittrich, J.; Le-Huu, M.; Mueller, M. M.; Bedke, J.; Kartenbeck, J.; Lehmann, W. D.; Krueger, R.; Bock, M.; Huss, R.; Seliger, C.; Gröne, H.-J.; Misselwitz, B.; Semmler, W.; Kiessling, F. *Invest. Radiol.* **2005**, *40*, 504−513.
(21) Harush-Frenkel, O.; Debotton, N.; Benita, S.; Altschuler, Y. *Biochem. Biophys. Res. Commun.* **2007**, *353*, 26−32.
(22) Dausend, J.; Musyanovych, A.; Dass, M.; Walther, P.; Schrezenmeier, H.; Landfester, K.; Mailänder, V. *Macromol. Biosci.* **2008**, *8*, 1135−1143.
(23) Harush-Frenkel, O.; Rozentur, E.; Benita, S.; Altschuler, Y. *Biomacromolecules* **2008**, *9*, 435−443.
(24) Arvizo, R. R.; Miranda, O. R.; Thompson, M. A.; Pabelick, C. M.; Bhattacharya, R.; Robertson, J. D.; Rotello, V. M.; Prakash, Y. S.; Mukherjee, P. *Nano Lett.* **2010**, *10*, 2543−2548.
(25) Liang, M.; Lin, I.-C.; Whittaker, M. R.; Minchin, R. F.; Monteiro, M. J.; Toth, I. *ACS Nano* **2010**, *4*, 403−413.
(26) Jiang, X.; Musyanovych, A.; Röcker, C.; Landfester, K.; Mailänder, V.; Nienhaus, G. U. *Nanoscale* **2011**, *3*, 2028−2035.
(27) Ma, J.; Chen, J. Y.; Zhang, Y.; Wang, P. N.; Guo, J.; Yang, W. L.; Wang, C. C. *J. Phys. Chem. B* **2007**, *111*, 12012−12016.
(28) Boldt, K.; Bruns, O. T.; Gaponik, N.; Eychmüller, A. *J. Phys. Chem. B* **2006**, *110*, 1959−1963.
(29) Aillon, K. L.; Xie, Y. M.; El-Gendy, N.; Berkland, C. J.; Forrest, M. L. *Adv. Drug Delivery Rev.* **2009**, *61*, 457−466.
(30) Mancini, M. C.; Kairdolf, B. A.; Smith, A. M.; Nie, S. *J. Am. Chem. Soc.* **2008**, *130*, 10836−10837.
(31) Kirchner, C.; Liedl, T.; Kudera, S.; Pellegrino, T.; Javier, A. M.; Gaub, H. E.; Stolzle, S.; Fertig, N.; Parak, W. J. *Nano Lett.* **2005**, *5*, 331−338.
(32) Bottrill, M.; Green, M. *Chem. Commun.* **2011**, *47*, 7039−7050.
(33) Chen, N.; He, Y.; Su, Y.; Li, X.; Huang, Q.; Wang, H.; Zhang, X.; Tai, R.; Fan, C. *Biomaterials* **2012**, *33*, 1238−1244.
(34) Chan, W. C. W.; Maxwell, D. J.; Gao, X.; Bailey, R. E.; Han, M.; Nie, S. *Curr. Opin. Biotechnol.* **2002**, *13*, 40−46.
(35) Michalet, X.; Pinaud, F. F.; Bentolila, L. A.; Tsay, J. M.; Doose, S.; Li, J. J.; Sundaresan, G.; Wu, A. M.; Gambhir, S. S.; Weiss, S. *Science* **2005**, *307*, 538−544.
(36) Bao, H.; Wang, E.; Dong, S. *Small* **2006**, *2*, 476−480.
(37) Ying, E.; Li, D.; Guo, S.; Dong, S.; Wang, J. *PloS One* **2008**, *3*, e2222.
(38) Röcker, C.; Pötzl, M.; Zhang, F.; Parak, W. J.; Nienhaus, G. U. *Nat. Nanotechnol.* **2009**, *4*, 577−580.
(39) Aldana, J.; Wang, Y. A.; Peng, X. *J. Am. Chem. Soc.* **2001**, *123*, 8844−8850.
(40) Gao, M.; Kirstein, S.; Möhwald, H.; Rogach, A. L.; Kornowski, A.; Eychmüller, A.; Weller, H. *J. Phys. Chem. B* **1998**, *102*, 8360−8363.
(41) Zhang, H.; Zhou, Z.; Yang, B.; Gao, M. *J. Phys. Chem. B* **2003**, *107*, 8−13.
(42) Jiang, X. E.; Röcker, C.; Hafner, M.; Brandholt, S.; Dörlich, R. M.; Nienhaus, G. U. *ACS Nano* **2010**, *4*, 6787−6797.
(43) Panté, N.; Kann, M. *Mol. Biol. Cell* **2002**, *13*, 425−434.
(44) Chen, M.; von Mikecz, A. *Exp. Cell Res.* **2005**, *305*, 51−62.